Study of normal incidence three component multilayer mirrors in the range 20 nm - 40 nm

Julien Gautier, Franck Delmotte, Marc Roulliay, Françoise Bridou,
Marie-Françoise Ravet-Krill, Arnaud Jérôme

Study of normal incidence of three-component multilayer mirrors in the range 20−40 nm

Julien Gautier, Franck Delmotte, Marc Roulliay, Françoise Bridou,
Marie-Françoise Ravet, and Arnaud Jérome

We study theoretically and experimentally the increase of normal incidence reflectivity generated by addition of a third material in the period of a standard periodic multilayer, for wavelengths in the range 20 to 40 nm. The nature and thickness of the three materials has been optimized to provide the best enhancement of reflectivity. Theoretical reflectivity of an optimized $B_4C/Mo/Si$ multilayer reaches 42% at 32 nm. $B_4C/Mo/Si$ multilayers have been deposited with a magnetron sputtering system and a reflectivity of 34% at 32 nm has been measured on a synchrotron radiation source. © 2005 Optical Society of America

OCIS codes: 340.7470, 310.1860.

1. Introduction

Classical extreme UV (EUV) multilayer mirrors consist of periodic stacks of two materials with a period thickness p deposited on a substrate. Owing to material absorption, the reflectivity of a periodic multilayer can be optimized by one's changing the respective thicknesses of the two materials within the period. In the optimized multilayer[1] the most absorbing material is thinner than $p/2$. In fact, by reduction of the thickness of the most absorbing material (t_{abs}), the absorption of one period is reduced, and the light penetrates deeper into the multilayer. But reducing t_{abs} also reduces the efficiency of each period (because it is no longer a quarter-wave stack). Thus there is a competition between the efficiency of each period and the number of efficient periods (which is limited by absorption).

 Different theoretical methods have been studied in order to improve multilayer reflectivity. Carniglia and Apfel in 1980 proposed a quasi-periodic structure in which p is kept constant but t_{abs} is varied through-

out the multilayer.[2] Basically, near the surface, t_{abs} is low to minimize absorption, and, near the substrate, t_{abs} is high (approximately $p/2$) to improve the reflectivity.[1]

Following this idea, Singh and Braat proposed to incorporate additional materials of differing complex refractive indices in various regions of the stack.[3] In fact, they added a third (and a fourth) material and made thicknesses of the three (or four) materials that were varied from one period to the next one: Less absorbing materials are mostly present near the surface, whereas most absorbing ones are located near the substrate. At a wavelength $\lambda = 13.4$ nm, the theoretical reflectivity of this new design reaches 78.1% as compared with 75.7% for a standard multilayer. The theoretical reflectance increase at this wavelength is only 3% in relative value.

With respect to the higher wavelength range ($\lambda > 50$ nm), Larruquert has developed a theory on quasi-periodic multicomponent multilayers made of highly absorbing materials[4,5] and established a rule of selection for the material to be used within a period in order to optimize the reflectivity. Unfortunately, this theory is no longer valid in the EUV range ($\lambda < 50$ nm) because most materials are only moderately absorbing. Nevertheless, Larruquert has proposed some examples of multicomponent multilayers in the EUV (at 30.4 and 50 nm) by using the same rule of selection. In theory, these structures provide high reflectivity increases, and the main increase happens when a third material is added to a classical multilayer.[6]

However, from a experimental point of view, to the authors' knowledge, quasi-periodic multicomponent multilayers have never been produced in the EUV range ($\lambda < 50$ nm). In fact, there are two major difficulties for producing such multilayers. The first one is the need to calibrate each material thickness, taking into account interfacial interdiffusion or intermixing that often occur during multilayer deposition. The second one is the lack of useful characterization means for such structures. So, making quasi-periodic multilayers seems not to be an efficient way to increase significantly the reflectivity as compared with the difficulties one has to overcome to produce such structures.

In the wavelength range 1.3 to 6.8 nm, Boher *et al.*[7] have studied theoretically and experimentally periodic structures with three or four materials. They demonstrated that, even with periodical structures, the addition of a third material can improve the reflectivity, and they proposed a material selection criteria.

Normal incidence mirrors for wavelengths ranging from 20 to 40 nm are of particular interest in the field of solar physics (EUV imaging telescopes) and new extreme ultraviolet (EUV) source developments (High Harmonic Generation sources, x-ray lasers, etc.). In this paper we focus on periodic multilayer structures, and we study theoretically and experimentally the increase of reflectance generated by the addition of a third material in the period for wavelengths in the range 20 to 40 nm. The first part deals with theoretical optimization of three-component periodical multilayers at $\lambda = 32$ nm. In the second part we explore the performances of these new multilayers ($B_4C/Mo/Si$) in the range $20-40$ nm. In the last part we present the experimental results obtained with three-component multilayers at $\lambda = 32$ nm.

2. Three-Component Multilayer Design at $\lambda = 32$ nm

In standard multilayers (with two components), the choice of materials depends on two decisive factors: Materials must have the highest index contrast, but materials and interfaces must also be chemically stable. Different two-component multilayer mirrors have already been produced for wavelengths between 20 and 40 nm, in particular Mo/Si,[8] B_4C/Si,[9,10] and Si_3N_4/Si[11] multilayers. These three kinds of multilayer present a good reflectivity, so a high contrast index is present between the two materials in this spectral region. Moreover, the aging and thermal stability of these structures have been reported to be satisfactory. For these reasons, we have selected Mo, Si, B_4C, and Si_3N_4 materials as good candidates to produce three-component multilayers.

In this part we theoretically study the possible reflectivity enhancement due to the addition of a third material in a standard multilayer. We have calculated the reflectivity of periodic multilayers with three materials per period at $\lambda = 32$ nm, and we have determined the material thicknesses that optimize the reflectivity. Each multilayer has 40 periods (more periods are useless owing to absorption). The reflec-

Table 1. Optical Constant at 32 nm and Density of B_4C, Mo, Si, Si_3N_4[a]

Materials	n	k	Density (g/cm^3)
B_4C	0.80527	0.06334	2.52
a-Si	0.92525	0.00926	2.19
Mo	0.96369	0.42567	10.22
Si_3N_4	0.81799	0.10454	3.44

For Si we use density of amorphous silicon, 94% of the density of crystalline Si.

tivity is calculated at normal incidence with the iterative method.[1] We make the hypothesis that the interfaces between adjacent layers are perfect; i.e., there are no scattering losses due to interface imperfections or compound formation. The optical constants of the four selected materials versus wavelength were calculated from the scattering factors of B, C, N,[12] Mo,[13] and Si[14] and are listed in Table 1 for $\lambda = 32$ nm. In this table, n is the real part of the index, and k is the absorption coefficient. The densities are also listed. A density of 2.19 g/cm^3 is taken for amorphous silicon, which represents 94% of the density of crystalline silicium. The density of the three other materials are the tabulated density. For convenience, we have also plotted these optical constants in the complex plane on Figure 1.

With these selected materials, we can make four triplets noted as (B_4C;Mo;Si), (Si_3N_4;Mo;Si), (B_4C;Si_3N_4;Si), and (B_4C;Mo;Si_3N_4). For each triplet we have to optimize the order of the materials in the stack and the nature of the top layer: There are six structure possibilities per triplet. For example, with the triplet (B_4C;Mo;Si) we can realize six multilayers noted as $B_4C/Mo/Si$, $B_4C/Si/Mo$, $Si/B_4C/Mo$, $Si/Mo/B_4C$, $Mo/Si/B_4C$, and $Mo/B_4C/Si$. In the notation $B_4C/Mo/Si$, the first material (B_4C) is on the top of the multilayer, and the last one (Si) is on the substrate. All the 24 combinations (six per triplet) must be optimized if we want to find the best design
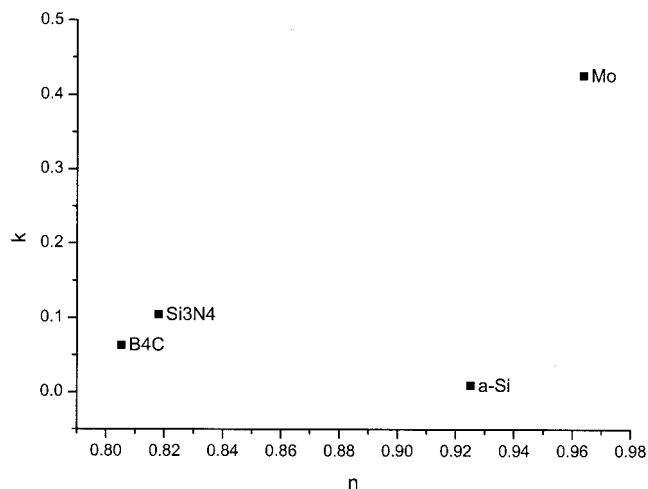

Fig. 1. Optical constants of B_4C, Mo, a-Si, and Si_3N_4 at 32 nm plotted in the complex index plane.

Table 2. Reflectivity (R) at 32 nm and Layer Thicknesses of Three-Component Multilayers Made of B_4C, Mo, and Si

	Optimal Order			Nonoptimal Order	
Structure	Thicknesses (nm)	R (%)	Structure	Thicknesses (nm)	R (%)
B_4C/Mo/Si	4.1/2.2/11.3	42.0	B_4C/Si/Mo	6.1/11.6/0	34.1
Mo/Si/B_4C	2.4/11.6/3.6	37.0	Mo/B_4C/Si	3.2/0/14.2	30.5
Si/B_4C/Mo	11.5/3.8/2.3	34.3	Si/Mo/B_4C	11.7/0/5.9	26.7

For each structure, the layer thicknesses have been calculated to optimize the reflectivity.

Fig. 2. Calculated reflectivity spectra of an optimized B_4C/Si multilayer (continus curve), an optimized B_4C/Mo/Si multilayer (dashed curve), and a multilayer made of the same stack in reverse order (Si/Mo/B_4C) (dotted curve) at the incidence angle of 0°.

because the multilayer reflectivity depends not only on the choice of the three materials but also on their order in the stack and on the nature of the top layer. For each combination the program numerically optimizes the thickness of each material for a wavelength and a number of period.

In Table 2 we present the results of reflectance optimization for the (B_4C;Mo;Si) triplet at λ = 32 nm. The six multilayers are classified into two columns. In the first one the addition of a third material increases the reflectivity: It is the optimal order column. In the second one the addition does not increase the reflectivity, and the optimization gives 0 –nm thickness for one material: In this nonoptimal order column, we find standard multilayers. Each line represents a different top layer: The B_4C top layer gives the best reflectivity, then Mo and Si. We can see that, for each top layer, a great increase of reflectivity is observed when the addition of a third material is in the good order. Concerning two-component multilayers, the best reflectivity is obtained for B_4C/Si and reaches 34.1%. The addition of Mo between B_4C and Si (Mo deposited on Si) allows an increase in reflectivity up to 42%, whereas the addition of Mo between Si and B_4C (Mo deposited on Si) gives no improvements. Thus the order of the stack in a three-component multilayer is crucial, as illustrated in Fig. 2. In this figure we compare the spectral response of three multilayers, calculated with IMD software.[15] The continuous curve is the simulation of a standard B_4C/Si multilayer optimized for λ = 32 nm (thicknesses are given in Table 2). The dashed curve is a simulation of the B_4C/Mo/Si multilayer previously optimized for λ = 32 nm (thicknesses are given in Table 2). The dotted curve represents the reflectivity of the same three-component multilayer with the same thicknesses but in reverse order: Si/Mo/B_4C. A relative increase of 23% can be observed in the optimal order (B_4C/Mo/Si) and a fall of 63% can be observed when we inverse the order of the stack (Si/Mo/B_4C).

Shown in Table 3 are the best results for the four triplets and the relative reflectivity increases obtained with three components instead of two. The first line is the same as the first line of Table 2. In the second column of Table 3, we present the best results of the standard multilayers. For all the triplets, the addition of a third material increases the reflectivity.
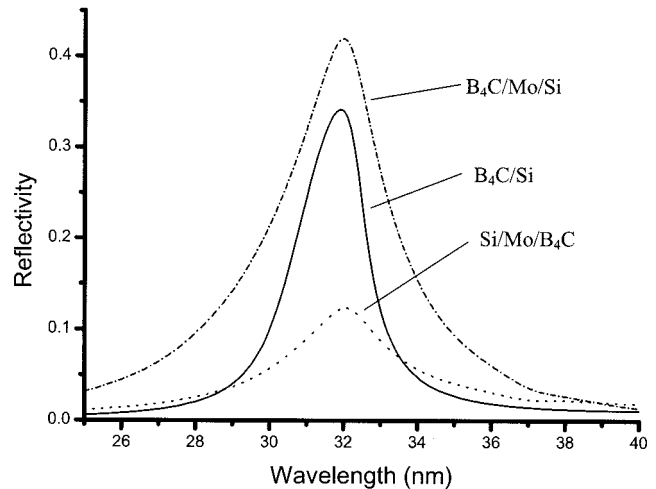
This enhancement is in relation with the index contrast between the third material and the materials of the standard multilayer (see Fig. 1). Indeed, for standard B_4C/Si multilayers the addition of Mo with a high contrast index increases the reflectivity to 23% (in relative values), whereas for Si_3N_4 (with a low index contrast) the increase is only 2.3%. For standard Mo/Si multilayers the addition of B_4C increases the reflectivity to 37.6% while the addition of Si_3N_4, which presents a lower contrast index, a relative increase of only 18% is observed.

We note that, for the first three examples shown in Table 3, the order of the stack satisfies both Larruquert's rule[6] (material index has to run clockwise in the complex plane represented on Fig. 1) and Boher's criterium[7] (the more absorbing material must be deposited on the less absorbing material). Nevertheless, for the last triplet (B_4C;Mo;Si_3N_4) the optimal structure B_4C/Mo/Si_3N_4 does not satisfy these selection rules. This shows that these two rules are not valid in the general case for wavelengths between 20 and 40 nm. This is, in fact, not really surprising. On the one hand, Boher's criterium is derived from a particular simulation study and is not supported by any theoretical calculation. On the other hand, the demonstration of Larruquert's rule is not valid for wavelengths below 50 nm.[6] However, concerning the selection of materials, Larruquert's selection rules and Boher's selection criteria can be used as a guide to find the optimal structure.

In conclusion, we observe by way of simulations that, in all cases, the addition of a third material can increase the reflectivity when the order of the stack is optimized. Concerning the selection of materials, it seems to be clear that, on a theoretical point of view, one has to choose materials with the highest optical index contrast for each material pair. Indeed, that is in agreement with Larruquert's selection rules and with Boher's selection criteria. As mentioned previ-

Table 3. Reflectivity (R) and Optimized Thicknesses for Three-Component Multilayers and Standard Multilayers

	Three-Component Multilayers				Standard Multilayers		
Structure	Thicknesses (nm)	R (%)	Relative Increase (%)		Structure	Thicknesses (nm)	R (%)
$B_4C/Mo/Si$	4.1/2.2/11.3	42.0	23.0		B_4C/Si	6.1/11.6	34.1
$Si_3N_4/Mo/Si$	2.7/2.5/12.3	36.2	18.4		Mo/Si	3.2/14.2	30.5
$B_4C/Si_3N_4/Si$	4.4/1.8/11.5	34.9	2.3		B_4C/Si	6.1/11.6	34.1
$B_4C/Mo/Si_3N_4$	5.9/6.2/6.6	16.1	28.8		B_4C/Mo	7.0/8.9	12.5

Best results for each triplet are reported.

ously, from an experimental point of view, one also has to take into account the stability of materials and interfaces, and this point provides an additional restriction to the theoretical possibilities.

Concerning the order of the material in the stack, Larruquert's rule or Boher's criterium failed to predict the optimal order in the general case, for wavelengths ranging from 20 to 40 nm. Owing to this lack of reliable rules for defining the optimal order, all possible combinations have to be explored in simulation to find the best design (i.e., optimal order and thicknesses of materials in the stack).

3. Three-Component $B_4C/Mo/Si$ Multilayer in the Range 20−40

In Section 2 we have show that $B_4C/Mo/Si$ three-component multilayers present the highest reflectivity at $\lambda = 32$ nm. In this part we study the theoretical performances of such a structure versus wavelength and versus the number of periods in the stack.

Figure 3 shows the calculated reflectance versus wavelength for the Mo/Si, B_4C/Si, and $B_4C/Mo/Si$ multilayers. For each wavelength, the design has been optimized with our program. For all kinds of multilayer, the reflectance decreases (as expected) when the wavelength increases far from the Si7 absorption edge at 12.4 nm. At 13 nm, when optimizing the three-component $B_4C/Mo/Si$ multilayer, we find
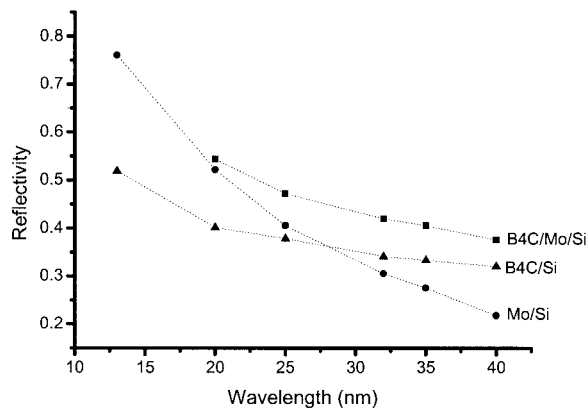
a standard Mo/Si multilayer (i.e., B4C thickness = 0). For all other wavelengths in the range 20 to 40 nm, we find an increase of reflectivity by using the three-component multilayer instead of standard Mo/Si or B_4C/Si multilayers.

The optimization of the reflectivity at $\lambda = 32$ nm versus the number of periods is shown in Fig. 4 for the $B_4C/Mo/Si$ three-component multilayer and the standard multilayer B_4C/Si. For each number of periods, we optimized material thicknesses in order to have the optimal reflectance at $\lambda = 32$ nm. In this graph we note that the number of periods (N) necessary to have 99% of the asymptotic reflectivity is lower for a three-component multilayer ($N = 14$) than for a standard multilayer ($N = 22$). This means that the number of layers (directly related to the number of interfaces) required to obtain 99% of the asymptotic reflectivity is approximately the same in both cases: 42 layers for the three-component multilayer and 44 for the standard multilayer. Nevertheless, the total thickness is lower for the three-component multilayer, so total absorption may be lower too, and reflectivity may be increased. Indeed, the great advantage of three-component multilayers
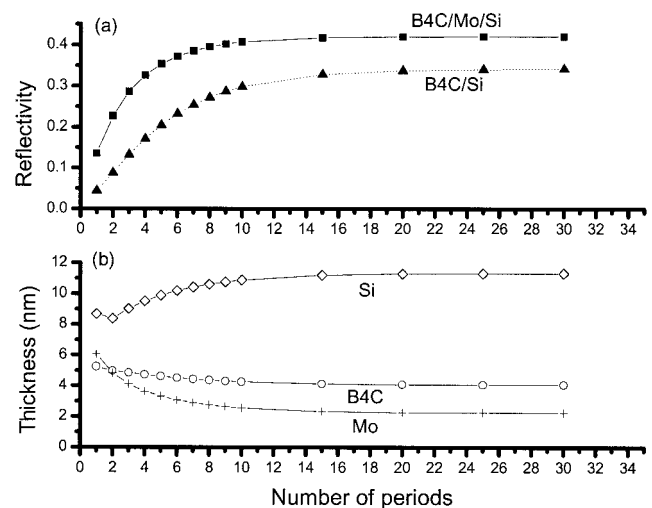

Fig. 3. Peak reflectance versus wavelength for Mo/Si (circles), B_4C/Si (triangles), and $B_4C/Mo/Si$ (squares) optimized multilayers. For each wavelength, the design has been optimized with our program.

Fig. 4. (a) Optimized reflectance of $B_4C/Mo/Si$ multilayer (squares) and B_4C/Si multilayer (triangles) versus number of periods in the stack. (b) Optimized thicknesses of Mo (crosses), B_4C (circles), and Si (rhombuses) corresponding to $B_4C/Mo/Si$ reflectance shown in (a) versus number of periods.
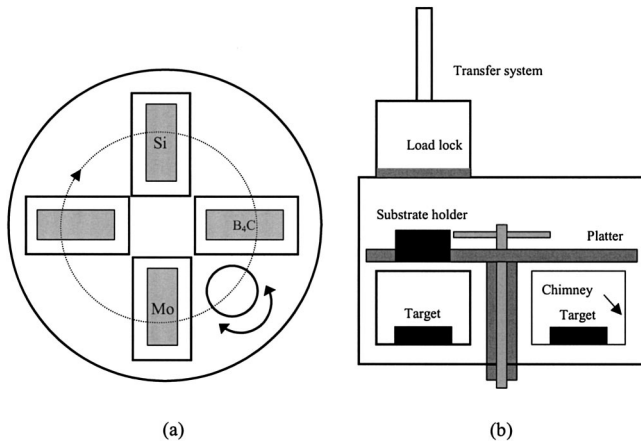
Fig. 5. Schematic of the magnetron sputtering deposition chamber: (a) top view and (b) side view.

Fig. 6. Grazing-angle reflectometry at 0.154 nm of a $B_4C/Mo/Si5$ multilayer: experimental data (dots) and fitted curve (solid curve).

is that this structure allows one to introduce more interfaces on a smaller thickness, which provides more contributions to the reflectance for the same absorption rate.

4. Three-Component $B_4C/Mo/Si$ Multilayer Fabrication and Characterization

Multilayers are deposited by use of a magnetron sputtering system equipped with four cathodes. The 80 mm × 200 mm rectangular targets are mounted in the bottom of the chamber with chimneys that limit the deposition region to the area directly above them. A background pressure of 2.7×10^{-6} Pa is obtained with a cryogenic pump. One deposits successive layers scanning the substrate above the target at a distance of 10 cm (Fig. 5). The thickness of each layer is controlled by the rotation velocity of the substrate on the target box (the motions are similar to those described by Montcalm *et al.*).[16] The typical velocity is adjusted from 0.2°/s to 2°/s. The substrate is rotating around its axis of symmetry at 50 rpm in order to obtain a good azimuthal uniformity.

During the process, we use a 0.27-Pa argon pressure in the deposition chamber. The plasma discharges are established with a rf power of 150 W for B_4C and Si targets and a dc of 0.19 A for the Mo target. The effective deposition rates for the different materials are indicated in Table 4. Multilayers are deposited onto 2-in. (1 in. = 2.54 cm) Si polished wafers.

After deposition, the multilayer structure is controlled by means of the grazing-incidence x-ray reflectometry at 0.154 nm.[17] By fitting the experimental
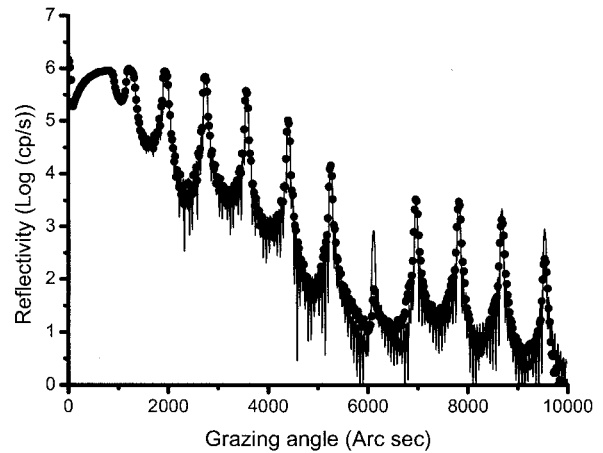
data we can deduce the period of the multilayer, the thicknesses of the different layers, the average interfacial roughnesses, and the material complex index at 0.154 nm. Several multilayers have been deposited and controlled, and one representative example is shown in Fig. 6 with a fitted curve. The different parameters of the fitted curve are shown in Table 5. Notice that all the Bragg peaks up to the 11th order are well defined on the experimental data: This shows that the multilayer periodicity is good. Moreover, all estimated interfacial rouhnesses reported in Table 5 are very low (less than 0.6 nm). On this example we fit a period of 17.6 nm with the following composition: d_{B_4C} = 4.2 nm, d_{Mo} = 2.2 nm, and d_{Si} = 11.2 nm (d_x represents the thickness of the material x). One can see that the index contrast between B_4C and Si is low at this wavelength, and this may induce a relative indetermination on the respective thicknesses of these two layers. However, simulations show that the reflectivity of three-component multilayers decreases only slightly when thicknesses are varied from the optimal calculated thickness.

Reflectance in the EUV range has been measured on the ELETTRA synchrotron radiation source. Measurements have been carried out on the Bending Magnet for Emission Absorption and Reflectivity (BEAR) beamline[18] with an incidence angle of 10 deg

Table 4. Effective Deposition Rates of Si, B_4C, and Mo Layers

Materials	rf Power (W)	dc Current (A)	Deposition Rate (nm/s)
Si	150	150	
Mo		0.19	
B_4C	0.11	0.014	0.13

Table 5. $B_4C/Mo/Si$ Multilayer Parameters Deduced from x-Ray Grazing-Angle Reflectometry Measurement

Layer	Thickness (nm)	Roughness (nm)	1-n (×10^{-6})	Absorption k (×10^{-6})
Si Substrate	∞	0.38	7.7	0.13
1−Si	11.2	0.52	7.28	0.13
2−Mo	2.67	0.41	25.95	1.68
3−B_4C	4.49	0.58	6.7	0.15
. . .				
60−B_4C	4.49	0.58	6.7	0.15

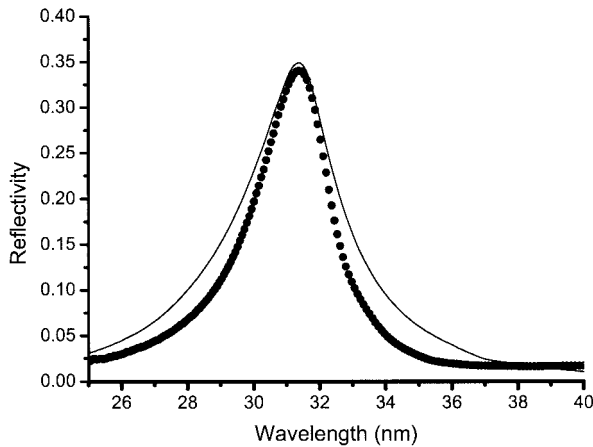[a]These parameters correspond to the fit curve of Fig. 6.

Fig. 7. Measured and calculated reflectivities of a B$_4$C/Mo/Si three-component multilayer at 10 deg in S polarization. Parameters of the simulated curve are given in the text.

(near normal incidence) in S polarization. We used a normal incidence monochromator with an energy resolution, $E/\Delta E$, above 2000 and a silicon photodiode detector. The experimental reflectance versus wavelength of a B$_4$C/Mo/Si multilayer is shown in Fig. 7. The period of this multilayer, deduced from grazing-incidence x-ray reflectometry measurements, is 18.1 nm.

We have measured a reflectance of 34%. This represents a relative increase of 29% as compared with the best reflectance obtained in this wavelength range (26.5% for Si/B$_4$C).[9] We have also plotted on Fig. 7 the curve calculated with thicknesses and roughnesses deduced from grazing-incidence x-ray reflectometry measurements. The experimental spectrum and the calculated one are in quite good agreement. However, differences in reflectance and bandpass can be seen, and the reasons for this discrepancy are still under investigation. Concerning long-term stability, we have measured on an ELETTRA synchrotron radiation source a B$_4$C/Mo/Si multilayer after eight months' storage in air: The peak reflectance is 34%, and the peak position has not shifted with time.

5. Conclusion

The optimization design, fabrication, and characterization of three-component periodic multilayers have been described. Simulations show that the use of a third material allows an important increase of the reflectance if the order of the three materials in the stack is optimized. Owing to their high reflectance and chemical stability in standard multilayers, we have selected in a theoretical study Mo, Si, B$_4$C, and Si$_3$N$_4$ materials as good candidates to produce three-component multilayers in the wavelength range 20 to 40 nm. The nature and thickness of the three materials have been optimized to provide the best enhancement of the calculated reflectivity. At $\lambda = 32$ nm, further enhancement is obtained by the optimization of a B$_4$C/Mo/Si multilayer (with B$_4$C is on the top and Si on the substrate). We obtain a calculated reflectivity of 42%, whereas the theoretical reflectivity of B$_4$C/Si (which is the best design with two materials for this wavelength) is only 34%. Simulations show that B$_4$C/Mo/Si multilayers are also promising for other wavelengths in the range 20 to 40 nm.

B$_4$C/Mo/Si multilayers with an optimized number of periods have been deposited with a magnetron sputtering system and characterized by x-ray grazing reflectometry and synchrotron radiation measurements. We obtained a experimental reflectivity of 34% at $\lambda = 32$ nm, which represents a relative increase of 29% as compared with the best standard multilayer reflectivity reported in the literature.

References

1. E. Spiller, *Soft X-Ray Optics* (SPIE, Bellingham, Wash., 1994).
2. C. K. Carniglia and J. H. Apfel, "Maximum reflectance of multilayer dielectric mirrors in the presence of slight absorption," J. Opt. Soc. Am. **70,** 523–534 (1980).
3. M. Singh and J. J. M. Braat, "Design of multilayer extreme-ultraviolet mirrors for enhanced reflectivity," Appl. Opt. **39,** 2189–2197 (2000).
4. J. I. Larruquert, "Reflectance enhancement with sub-quarterwave multilayers of highly absorbing materials," Opt. Soc. Am. A **18,** 1406–1414 (2001).
5. J. I. Larruquert, "New layer-by-layer multilayer design method," Opt. Soc. Am. A **19,** 385–390 (2002).
6. J. I. Larruquert, "Reflectance enhancement in the extreme ultraviolet and soft x rays by means of multilayers with more than two materials," Opt. Soc. Am. A **19,** 391–397 (2002).
7. P. Boher, L. Hennet, and Ph. Houdy, "Three materials soft x-ray mirrors: theory and application," in *Advanced X-Ray/EUV Radiation Sources and Applications*, J. P. Knaueur and G. K. Shenoy, eds., Proc. SPIE **1345,** 198–212 (1990).
8. M. F. Ravet, F. Bridou, X. Zhang-Song, A. Jerome, F. Delmotte, R. Mercier, M. Bougnet, P. Bouyries, and J. P. Delaboudiniere, "Ion beam deposited Mo/Si multilayers for EUV imaging applications in astrophysics," in *Advances in Optical Thin Films*, C. Amra, N. Kaiser, and H. Macleod, eds., Proc. SPIE **5250,** 99–108 (2004).
9. D. L. Windt, S. Donguy, J. Seely, B. Kjornrattanawanich, E. Mgullikson, C. C. Wlton, L. Golub and E. DeLuca, "EUV multilayers for solar physics," in *Optics for EUV, X-Ray, and Gamma-Ray Astronomy*, O. Citterio and S. L. O'Dell, eds., Proc. SPIE **5168,** 1–11 (2004).
10. F. Delmotte, M. F. Ravet, F. Bridou, X. Song, A. Jerome, S. Boujdayane, S. Hubert, P. Zeitoun, M. Idir, and P. Troussel, "Depot et calibration de multicouches pour l'optique XUV dans la gamme 10−30 nm," J. Phys. IV France **108,** 255–258 (2003).

11. P. Boher, Ph. Houdy, L. Hennet, P. Müller, Z. G. Li, and D. J. Smith, "Silicon/silicon oxide and silicon/silicon nitride multilayers for extreme ultraviolet optical applications," Opt. Eng. **30,** 1049–1060 (1991).

12. B. L. Henke, E. M. Gullikson, and J. C. Davis, "X-ray interactions: photoabsorption, scattering, and reflection at $E = 50–30000$ eV, $Z = 1–92$," At. Data Nucl. Data Tables **54,** 181–342 (1993).

13. R. Soufli and E. M. Gullikson, "Absolute photoabsorption measurements of molybdenum in the range 60 to 930 eV for optical constant determination," Appl. Opt. **37,** 1713–1719 (1998).

14. R. Soufli and E. M. Gullikson, "Reflectance measurement on clean surfaces for the determination of optical constants of materials in the EUV/soft x ray region," Appl. Opt. **36,** 5499–5507 (1997).

15. IMD software developed by David Windt, see http://cletus.phys.columbia.edu/~win.

16. C. Montcalm, S. Bajt, P. B. Mirkarimi, E. Spiller, F. J. Weber, and J. A. Folta, "Multilayer reflective coatings for extreme-ultraviolet lithography," in *Emerging Lithographic Technologies II*, Y. Vladimirsky, ed., Proc. SPIE **3331,** 42–50 (1998).

17. F. Bridou and B. Pardo, "Automatic characterization of layers stacks from reflectivity measurments. Application to the study of the validity conditions of the grazing X-rays reflectometry," J. Optics (Paris) **21,** 183–191 (1990).

18. F. Borgatti, A. De Luisa, B. Doyle, A. Giglia, N. Mahne, I. Pasquali, M. Pedio, G. Selvaggi, S. Nannarone, G. Naletto, M. G. Pelizzo, and G. Tondello, "The new Bear beamline: a short presentation," elettra news 47(2003), see http://www.elettra.trieste.it/science/elettranews/volume47/en117.html.